Academic Journal of Science and Technology
ISSN: 2771-3032 | Vol. 14, No. 1, 2025

The Investigation of Fault Slip Mechanisms During Hydraulic Fracturing in Horizontal Shale Gas Wells

Zixian Guo[1, 2, 3], Yang Li[1, 2, 3]

[1]School of Mechanical Engineering, Southwest Petroleum University, Chengdu, Sichuan 610500, China
[2]State Key Laboratory of Shale Oil and Gas Enrichment Mechanisms and Effective Development, Beijing 100080, China
[3]State Energy Center for Shale Oil Research and Development, Beijing 100020, China

Abstract: Fault slip is the primary cause of casing deformation during the hydraulic fracturing process of shale gas horizontal wells. This paper investigates the mechanism of fault slip and its correlation with the integrity of the cement sheath. By establishing a numerical model of the casing-cement sheath-reservoir rock system, the effects of fracturing fluid pressure and temperature, mechanical parameters of the cement sheath, and the wall thickness of the casing and cement sheath on the integrity of the cement sheath were calculated. The results indicate that low-temperature fracturing fluids lead to changes in the stress state at the casing-cement sheath interface and the reservoir rock-cement sheath interface, with failure at the casing-cement sheath interface occurring approximately 600s after exposure. Increasing the temperature of the fracturing fluid, selecting a cement sheath with a lower elastic modulus and higher Poisson's ratio, and increasing the casing wall thickness can effectively enhance the integrity of the casing-cement sheath-reservoir rock system and prevent fault slip induced by fracturing fluids.

Keywords: Fault slip; Shale gas; Hydraulic fracturing; Cement sheath; Integrity.

1. Introduction

In the process of volume modification for shale gas horizontal wells, casing deformation is a common occurrence. As of April 2019, the overall casing deformation rate in the Weiyuan block was approximately 57.7%, with the Changning block at 31.9% and the Zhaotong block at 22.5%. By December 2022, the casing deformation rate in the Southern Sichuan Luzhou block was about 51.0%, with the Lu203 well area reaching a high of 68.6%[1–3]. A consensus has been reached on the mechanism of casing deformation: during hydraulic fracturing, faults intersecting the wellbore slip, causing localized reduction in casing diameter[4–7]. However, the specific causes of fault slip induced during fracturing are not well understood. Chen et al.[8], by integrating ant body tracking of fracture positions and well logging interpretations, found that casing deformations occur in areas adjacent to strongly developed fractures, suggesting that high-volume fracturing operations create artificial fractures that communicate with faults, inducing slippage. Zhang et al.[9] argue that in heterogeneous shale, the initiation and propagation of multiple hydraulic fractures lead to non-uniform stress accumulation around the wellbore, triggering fault slip. Li et al.[10] believe that the expansion of hydraulic fractures alters the local stress field, thereby changing the mechanical balance of faults and activating them. However, Han et al.[2], through extensive microseismic monitoring in the study area, found that casing deformation points are generally far from the target fracturing sections, often hundreds to thousands of meters away. This indicates that, under these circumstances, the communication of artificial fractures with faults and stress changes due to fracturing are unlikely to be the primary controlling factors for inducing fault slip. Zhang et al.[11] were the first to mention that fracturing fluid may enter faults through micro-annuli in the cement sheath, thereby inducing slippage.

In summary, a substantial body of research has focused on the two factors that induce fault slip: the communication of artificial fractures with faults and the stress changes caused by hydraulic fracturing[12–17]. While these factors can account for casing deformations occurring in the vicinity of the fracturing area, they fail to explain deformations at points far from the fracturing zone. Therefore, the infiltration of fracturing fluid into faults through micro-annuli in the cement sheath is likely a primary controlling factor for fault slip at these distant locations. Building on previous studies, this paper will use numerical simulations to further investigate the debonding of the cement sheath during hydraulic fracturing, which allows fracturing fluid to flow through this pathway into the fault, explaining the occurrence of fault slip at distances from the fracturing area. Additionally, this study will propose mitigation measures to prevent the entry of fracturing fluid into faults.

2. Mode of Fracturing Fluid Entering Fault

Faults intersecting with wellbores in the formation can lead to complications during hydraulic fracturing. When fracturing fluid is injected into the casing at low temperatures, it is transmitted to the casing-cement sheath-reservoir rock system, causing radial contraction and leading to the failure of the cement sheath. This can result in debonding at the casing-cement sheath interface or the cement sheath-reservoir rock interface, creating fluid pathways. During the construction process, when fracturing fluid is injected through perforation holes, it follows these pathways, entering and potentially inducing shear slippage along the faults, as depicted in Fig 1. Consequently, studying the mechanism of fault slip during hydraulic fracturing can be transformed into a study of the integrity of the cement sheath.

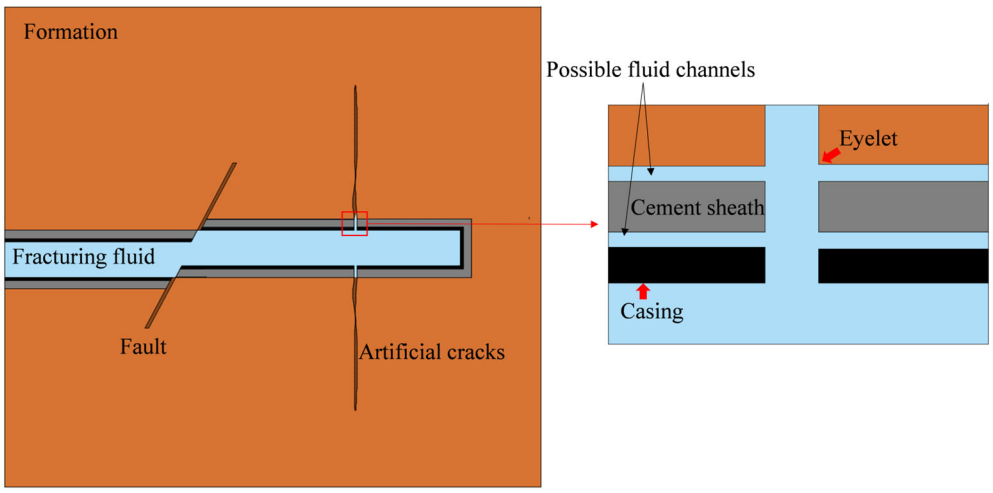

Figure 1. Schematic diagram of fracturing fluid entering fault

3. Calculation Method and Cement Sheath Failure Criterion

3.1. Governing equations

The heat transfer between the casing-cement sheath-formation is a form of solid-state heat transfer, and the thermal conduction equation is given as follows[18]:

$$\frac{\partial T}{\partial t}=a_j\left(\frac{\partial^2 T}{\partial r^2}+\frac{1}{r_j}\frac{\partial T}{\partial r}+\frac{\partial^2 T}{\partial z^2}\right)+\frac{Q_{vj}}{c_j\rho_j} \tag{1}$$

In the equation, T represents the temperature of the heat-conducting solid, in °C; t denotes the time of heat conduction, in seconds; $a_j=\frac{\lambda_j}{c_j\rho_j}$, a_j is the thermal diffusivity, in m²/s; c_j is the specific heat capacity, in J/(kg·°C); ρ_j is the density, in kg/m³; r_j is the radial distance, in meters; z is the axial distance along the wellbore, in meters; λ_j is the thermal conductivity, in W/(m·°C); and Q_{vj} is the heat absorbed or released per unit volume of the solid per unit time, in W.

When $j=1$ represents the casing properties, $Q_{v1}=Q_c$ denotes the convective heat transfer between the casing inner wall and the fracturing fluid. When $j=2$ represents the cement sheath properties, and When $j>1$ are $Q_{vj}=0$. When $j>2$ represents the reservoir rock properties, the parameters pertain to the formation.

The convective heat transfer coefficient, which characterizes the heat exchange capacity between a fluid and a solid surface, is closely related to the fluid's velocity. Consequently, the impact of the fracturing fluid's flow rate must be considered[19]. The convective heat transfer coefficient is determined by the following formula[20]:

$$\alpha=\frac{S_t\bullet K_f}{d} \tag{2}$$

In the equation, S_t represents the Stanton number, which is dimensionless; K_f denotes the thermal conductivity of the fracturing fluid, in W/(m·°C).

During the hydraulic fracturing process, the flow regime of the fluid within the casing is as follows:

$$\mathrm{Re}=\frac{\rho v d}{\mu} \tag{3}$$

In the equation, Re denotes the Reynolds number, which is dimensionless; ρ represents the density of the fracturing fluid, in kg/m³; v signifies the velocity of the fracturing fluid, $v=\frac{4Q}{\pi d^2}$, in m/s; d is the inner diameter of the casing, in meters; μ denotes the dynamic viscosity of the fracturing fluid, in Pa·s; and Q represents the flow rate of the fracturing fluid, in m³/min.

Based on the Reynolds number, it can be determined that the flow regime of the fracturing fluid within the casing during hydraulic fracturing is turbulent[21]. The Stanton number for turbulent flow conditions is calculated using the following formula:

$$S_t=0.0107\,\mathrm{Re}^{0.67}\,\mathrm{Pr}^{0.33} \tag{4}$$

In the equation, $\mathrm{Pr}=\frac{\gamma C_f}{K_f}$, Pr denotes the Prandtl number, which is dimensionless. γ represents the apparent viscosity of the fracturing fluid, in Pa·s; C_f denotes the specific heat capacity of the fracturing fluid, in J/(kg·°C).

Thus, the relationship between the fracturing fluid flow rate

and the heat transfer coefficient is derived as follows:

$$\alpha = \frac{0.012584\rho^{0.67}\gamma^{0.33}C_f^{\ 0.33}K_f^{\ 0.67}}{d^{1.67}\mu^{0.67}}Q^{0.67} \tag{5}$$

According to the superposition principle, the stress conditions at the interfaces within the casing-cement sheath-reservoir rock system during hydraulic fracturing, which result from the combined effects of pressure loads and thermal stress loads, are as follows[22]:

$$\begin{cases} \left(\sigma_r^t\right)_i = \left(\sigma_r\right)_i + \left(\sigma_r\right)_i^{'} \\ \left(\sigma_\theta^t\right)_i = \left(\sigma_\theta\right)_i + \left(\sigma_\theta\right)_i^{'} \end{cases} \tag{6}$$

In the equation, $i = 1$ represents the radial stress at the casing-cement sheath interface, and $i = 2$ represents the radial stress at the formation-cement sheath interface; $\left(\sigma_r\right)_i$ denotes the hoop stress at the i interface, and $\left(\sigma_\theta\right)_i$ denotes the hoop stress at the i interface; both are in MPa. $\left(\sigma_r\right)_i^{'}$ is the radial stress due to temperature changes, in MPa, and $\left(\sigma_\theta\right)_i^{'}$ is the hoop stress due to temperature changes, also in MPa.

3.2. Cement sheath failure criterion

In actual hydraulic fracturing operations, the cement sheath is often subjected to a combination of compressive and tensile stresses[23]. Consequently, to more accurately assess the damage to the cement sheath, the Mohr-Coulomb failure criterion has been introduced, as shown in Tab 1.Based on this criterion and integrating previous research findings, the stress relationships in cylindrical coordinates are confirmed as follows[24]: $\sigma_1 = \sigma_\theta$, $\sigma_3 = \sigma_r$, where σ_θ and σ_r represent the hoop and radial stresses in the cement sheath, respectively, in MPa. Concurrently, according to the experimental results of Zeng Bo et al.[25], σ_c is determined to be 40.5 MPa and σ_t is 3.5 MPa.

Table 1. Mohr Coulomb failure criterion

Stress interval	Interval description	Principal stress relation	Failure criteria
1	Stretch-stretch-stretch	$\sigma_1 \geq \sigma_3 \geq 0$	$\sigma_1 \geq \sigma_t$
2	Compression-compression-compression	$0 \geq \sigma_1 \geq \sigma_3$	$-\sigma_3 \geq \sigma_c$
3	Stretch-compression-compression, stretch-stretch-compression	$\sigma_1 \geq 0 \geq \sigma_3$	$\frac{\sigma_1}{\sigma_t} - \frac{\sigma_3}{\sigma_c} \geq 1$

Note: σ_1 and σ_3 represent the maximum and minimum principal stresses in the cement sheath, respectively, in MPa; σ_t denotes the tensile strength of the cement sheath, in MPa; and σ_c signifies the compressive strength of the cement sheath, also in MPa.

4. Numerical Model and Calculation Results

4.1. Numerical model

Due to the excessive number of elements in the 3D finite element model of the horizontal section, which leads to slow computational efficiency and high time costs, and considering that the axial length of the casing is much greater than its diameter, this study employs a 2D plane finite element model in place of the 3D model. Fig 2 illustrates the geometric shape of the casing-cement sheath-reservoir rock system model. To mitigate boundary effects, the entire model is sized at 10m×10m, with the cement sheath having an outer diameter of 0.2159m, the casing an outer diameter of 0.1778m, and an inner diameter of 0.1562m. Cohesive contact is set at the cement sheath-casing interface and the cement sheath-reservoir rock interface, with specific parameters detailed in Tab 2. The finite element simulation software uses temperature-displacement coupled elements CPE4T to discretize the reservoir rock, cement sheath, and casing. The initial temperature and initial in situ stress of the casing-cement sheath-reservoir rock system are set using a predefined field method, and pressure and thermal exchange conditions are applied to the inner wall of the casing. Displacements in the x and y directions at the model boundaries are restricted, with specific boundary condition values provided in Tab 3. To obtain the initial stress state of the cement sheath at the onset of hydraulic fracturing, this study accounts for the time-varying elastic modulus of the cement sheath during the cementing stage, setting a lower modulus at the initial stage of cementing, which is then increased. The material parameters for the model are sourced from open-access literature[26], as detailed in Tab 4.

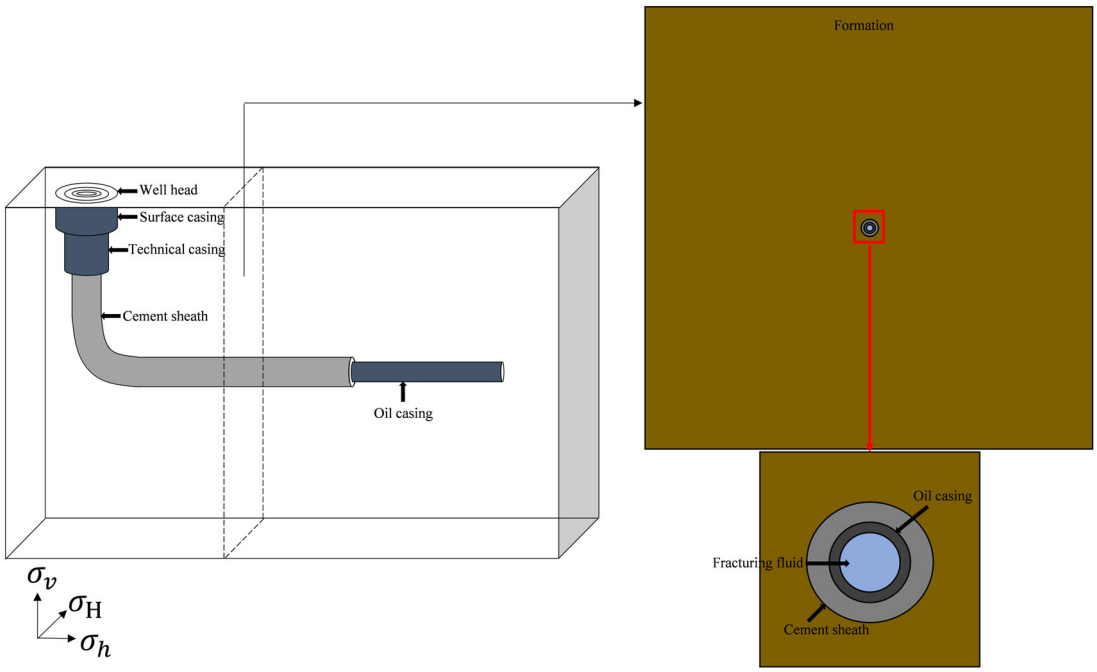

Figure 2. Numerical model of casing-cement sheath-formation system

Table 2. Interface contact properties

	Tensile bond strength, MPa	Shear bond strength, MPa	Cohesive stiffness, MPa	Fracture energy, J/m^2
Formation-cement sheath interface	0.42	0.42	3e4	100
Casing-cement sheath interface	0.5	2	3e4	100

Table 3. Model boundary conditions

Parameter	Units	Value
Maximum horizontal stress	MPa	95
Minimum horizontal stress	MPa	85
Vertical stress	MPa	90
Casing internal pressure during cementing	MPa	40
Casing internal pressure during fracturing	MPa	90
Initial stress of cement sheath	MPa	50
Fracturing fluid temperature	℃	20
Initial temperature of casing-cement sheath-formation system	℃	100

Table 4. Model material parameters

Parameter	Units	Casing	Cement sheath	Formation
Thermal conductivity	W/m/K	50.0	1.0	2.1
Density	kg/m^3	7800	3100	2240
Modulus of elasticity	GPa	210	8	22
Poisson's ratio		0.30	0.15	0.30
Coefficient of expansion	m/m/K	1.2e^{-5}	1e^{-5}	7.9e^{-6}
Specific heat capacity	J/kg/k	450	1600	1256

4.2. Base Case

In the baseline case study, the temperature variations of the casing-cement sheath-reservoir rock system during the hydraulic fracturing of shale gas wells were analyzed, as illustrated in Fig 3a and Fig 4. It was observed that with the injection of low-temperature fracturing fluid, the temperature of the outer wall of the casing rapidly decreased to approximately 20°C due to its good thermal conductivity. Simultaneously, the temperature of the cement sheath was

also affected by the low temperature; as the fracturing fluid continued to be injected, the overall temperature of the cement sheath gradually declined. Given the generally lower thermal conductivity of the cement sheath, a temperature gradient developed between its inner and outer walls, with the outer wall being warmer than the inner wall. This raises concerns that the casing-cement sheath interface may be more significantly impacted by the low temperature, thereby increasing the likelihood of failure.

To validate the aforementioned hypothesis, the stress variations at the casing-cement sheath interface and the reservoir rock-cement sheath interface during the cementing and hydraulic fracturing processes were analyzed, as depicted in Fig 3b and Fig 5. During the cementing phase, as the cement slurry is pumped in, the internal stress of 50 MPa within the slurry exceeds the drilling fluid pressure of 40 MPa, typically due to the higher density of cement slurry compared to water. The cement sheath, influenced by the in situ stress of the formation during solidification, exhibits compressive stresses in both radial and hoop directions at both interfaces, which decrease as the elastic modulus of the cement sheath increases. In the fracturing phase, the stress conditions at both interfaces change: ① At the cement sheath-reservoir rock interface, the radial stress becomes negative, indicating compressive stress. It initially decreases and then increases due to the initial contraction caused by the low-temperature fracturing fluid, followed by an increase in radial compressive stress as the pressure of the fracturing fluid leads to slight deformation of the casing, compressing the cement sheath. Once the fracturing fluid pressure stabilizes, the compressive stress levels off. The hoop stress remains in a compressive state. ② At the casing-cement sheath interface, the radial stress trend is consistent with the other interface but with a more significant variation, attributed to the lower temperature and greater contraction at this interface, resulting in higher radial compressive stress. As the fracturing fluid is injected, the hoop stress transitions from compressive to tensile and gradually increases, due to the decreasing temperature on the inner wall of the cement sheath, which causes an increase in hoop stress

Analyzing stress variations at the two interfaces alone is insufficient to determine whether the cement sheath has failed; hence, the Mohr-Coulomb failure criterion is employed to assess the failure state of the cement sheath. As shown in Fig 3c, it can be observed that at the reservoir rock-cement sheath interface, the Mohr-Coulomb failure value remains less than 1 throughout the fracturing process, indicating no failure at this interface. In contrast, at the casing-cement sheath interface, the Mohr-Coulomb failure value exceeds 1 approximately 500s after the onset of fracturing, signifying failure of the cement sheath. This suggests that debonding of the cement sheath at this interface has occurred, creating a fluid pathway.

To comprehensively assess the potential failure of the cement sheath interface under various conditions, a thorough investigation of the key parameters influencing the debonding of the cement sheath will be conducted next.

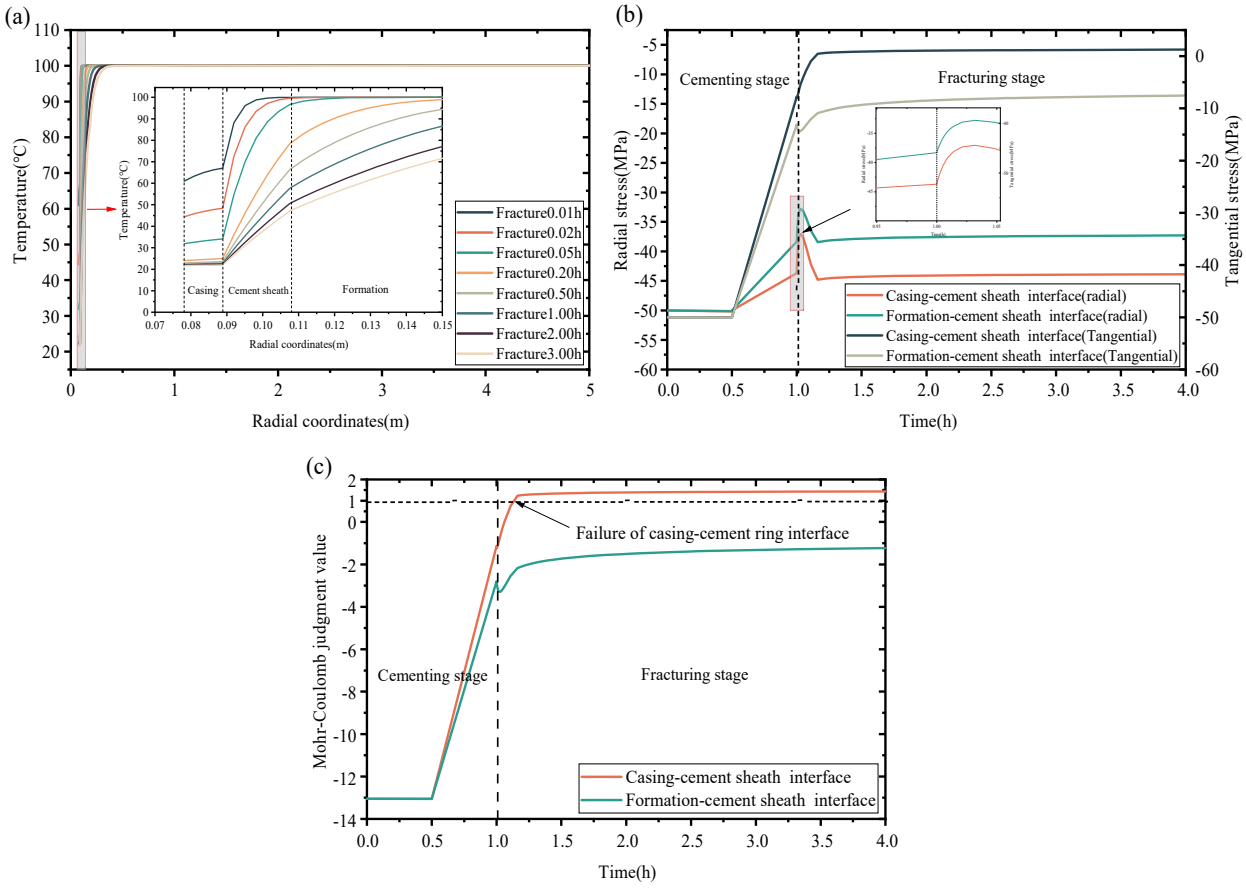

Figure 3. (a). Temperature changes of casing cement sheath formation system during fracturing; (b) The stress changes of the two interfaces at different stages; (c) Failure judgment of cement sheath interface

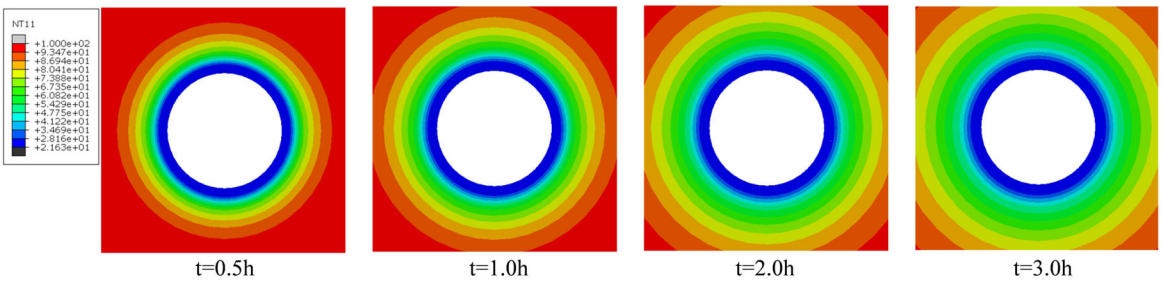

Figure 4. Temperature distribution of casing cement sheath formation system at different times

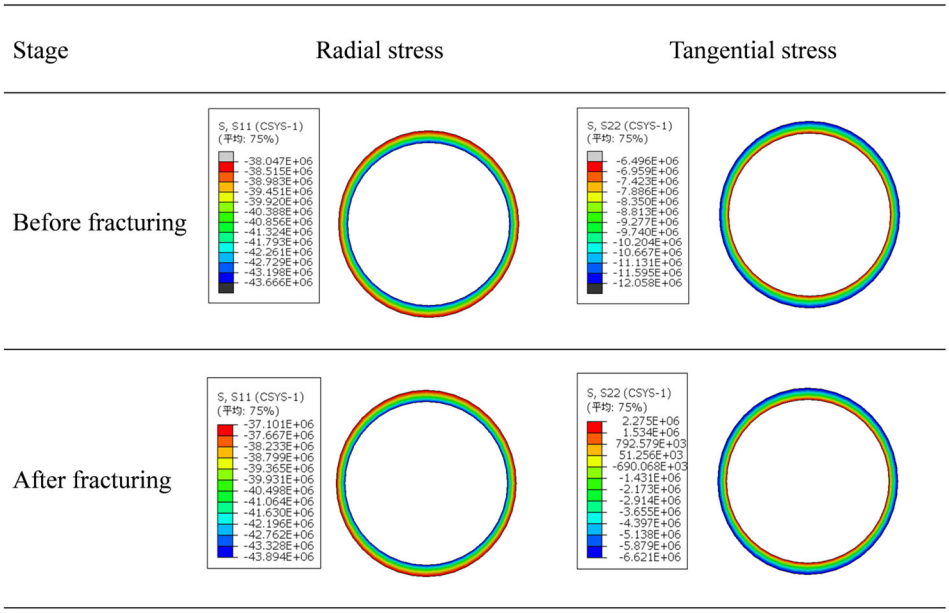

Figure 5. Stress changes of cement sheath before and after fracturing

4.3. Analysis of influencing factors

The integrity of the cement sheath during the hydraulic fracturing process may be influenced by factors such as fracturing fluid pressure and temperature, the mechanical properties of the cement sheath, and the wall thickness of the casing and cement sheath. To further identify the critical parameters, it is necessary to conduct a sensitivity analysis of these factors. Moreover, from the baseline case study, it is known that there is a risk of failure at the casing-cement sheath interface during the fracturing process; hence, this section focuses on the failure assessment at the casing-cement sheath interface.

4.3.1. Fracturing fluid pressure and temperature

During the construction process, the pressure of the fracturing fluid fluctuates[27], and the fluid pressure during fracturing is typically 5 to 20 MPa higher than the minimum horizontal stress. To investigate the impact of varying fracturing fluid pressures on the integrity of the cement sheath, this section conducts an analysis with fracturing fluid pressures set at 90, 95, 100, and 105 MPa, while all other parameters remain consistent with the baseline case. Fig 6a illustrates the failure assessment at the casing-cement sheath interface under different fracturing fluid pressures. It can be observed that during the fracturing stage, failure at the casing-cement sheath interface occurs under all tested pressures, and the higher the fracturing fluid pressure, the greater the Mohr-Coulomb failure value, indicating earlier failure at the interface. This is attributed to the fact that higher fracturing fluid pressures, although causing less deformation in the casing, subject the cement sheath to higher stress, and literature suggests that cement is more prone to failure under high stress conditions[28].

From the baseline case study, it is evident that the temperature of the fracturing fluid significantly affects the casing-cement sheath-reservoir rock system; hence, it is essential to analyze the failure risk at the casing-cement sheath interface under various fracturing fluid temperatures. The fracturing fluid temperatures were set to 20, 40, 60, and 80°C, with all other parameters held constant as in the baseline scenario. Fig 6b presents the failure assessment at the casing-cement sheath interface under different fracturing fluid temperatures. It can be observed that higher fracturing fluid temperatures result in lower Mohr-Coulomb failure values, delaying the time at which failure occurs at the casing-cement sheath interface. When the fracturing fluid temperature is 80°C, the Mohr-Coulomb failure value remains below 1 throughout the entire fracturing process, indicating no failure at the interface. Therefore, increasing the fracturing fluid temperature can effectively reduce the risk of cement sheath failure and enhance the integrity of the casing-cement sheath-reservoir rock system.

Fig 7 illustrates the impact of fracturing fluid pressure and temperature on the failure time of the cement sheath. It is evident that higher fracturing fluid pressure and lower temperature lead to a more rapid failure at the casing-cement sheath interface. Specifically, when the pressure is 105 MPa and the temperature is 20°C, failure occurs at the interface

after approximately 350s of fracturing.

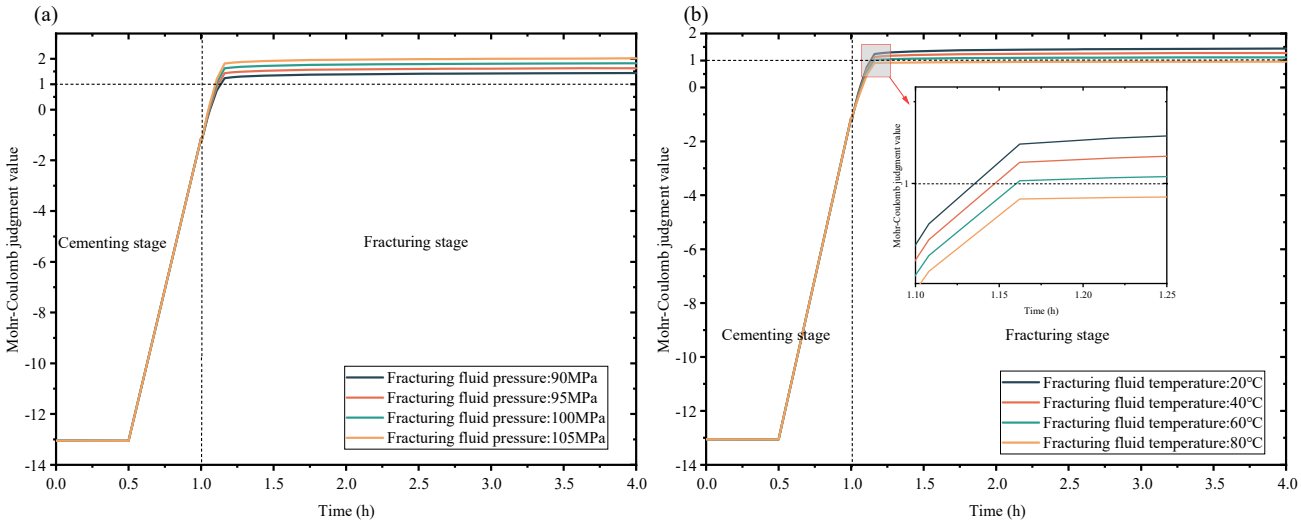

Figure 6. (a) Failure judgment of casing cement sheath interface under different fracturing fluid pressures; (b) Failure judgment of casing cement sheath interface under different fracturing fluid temperatures

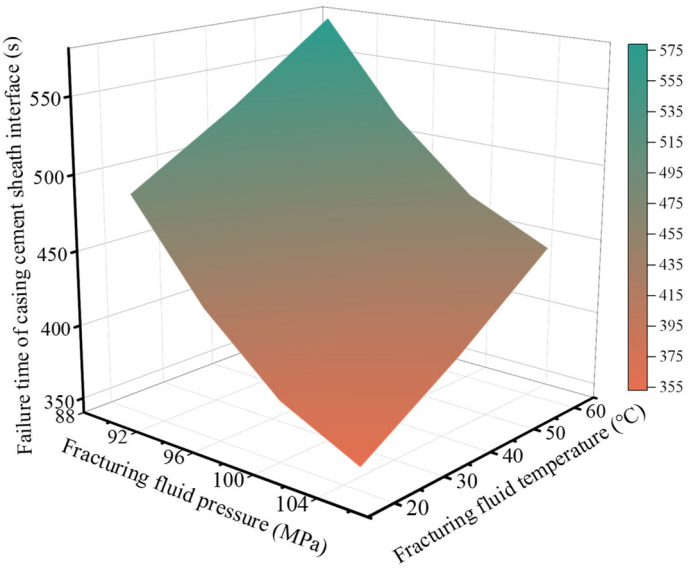

Figure 7. Influence of fracturing fluid pressure and temperature on cement sheath failure time

4.3.2. Elastic modulus and Poisson's ratio of cement sheath

This section investigates the impact of the cement sheath's elastic modulus on its integrity. The elastic modulus of the cement sheath was set to 6, 8, 10, and 12 GPa, with all other parameters held constant as in the baseline case. Fig 8a presents the failure assessment at the casing-cement sheath interface under different elastic moduli of the cement sheath. It is observed that during the cementing phase, variations in the elastic modulus have a minimal impact on the Mohr-Coulomb failure value. In contrast, during the fracturing phase, a lower elastic modulus correlates with a lower failure value, resulting in a slower failure rate at the casing-cement sheath interface. When the elastic modulus of the cement sheath is 6 GPa, no failure occurs at the interface during the fracturing phase. This indicates that reducing the elastic modulus of the cement sheath can effectively ensure its integrity.

This section also examines the impact of the Poisson's ratio of the cement sheath on its integrity, with the Poisson's ratio set to 0.10, 0.15, 0.20, and 0.25 for the cement sheath. All other parameters are consistent with the baseline case. Fig 8b displays the failure assessment at the casing-cement sheath interface under various Poisson's ratios. It is observed that the Poisson's ratio significantly affects the integrity of the casing-cement sheath interface; as the Poisson's ratio increases, the Mohr-Coulomb failure value decreases. When the Poisson's ratio is 0.20 and 0.25, no failure occurs at the casing-cement sheath interface during the fracturing stage. In summary, selecting a combination of low elastic modulus and high Poisson's ratio for the cement slurry system can effectively enhance the integrity of the casing-cement sheath-reservoir rock system during hydraulic fracturing.

Fig 9 depicts the influence of the cement sheath's elastic modulus and Poisson's ratio on its failure time. It is observed that a higher elastic modulus and a lower Poisson's ratio of

the cement sheath lead to a more rapid failure at the casing-cement sheath interface. Specifically, when the elastic modulus is 12 GPa and Poisson's ratio is 0.10, failure at the interface occurs after approximately 100s of fracturing.

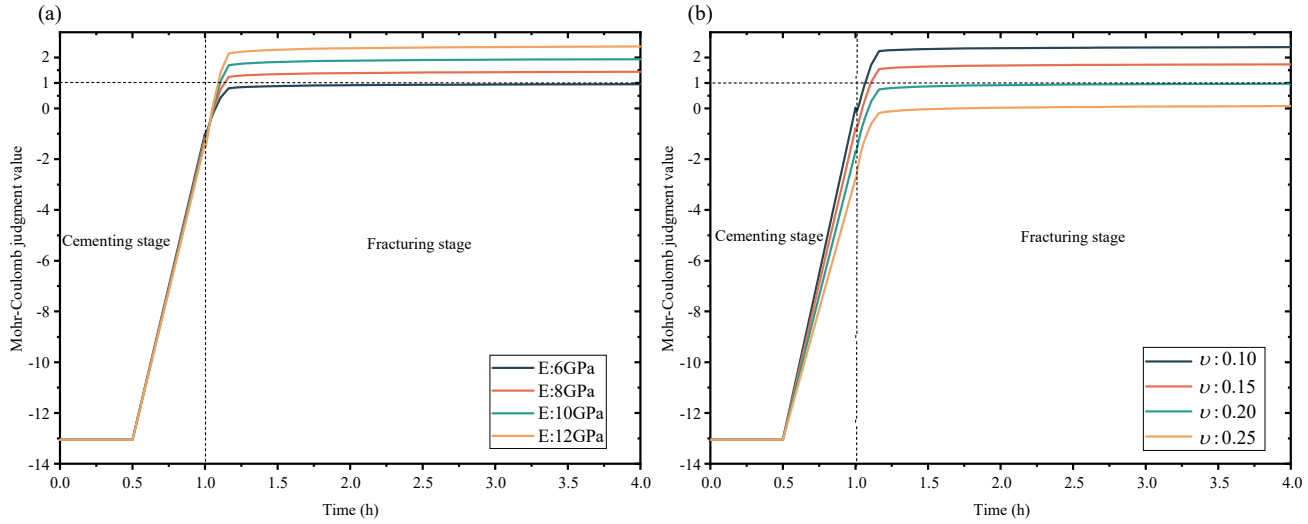

Figure 8. (a) Failure judgment of casing cement sheath interface under different elastic modulus of cement sheath; (b) Failure judgment of casing cement sheath interface under different cement sheath Poisson's ratio

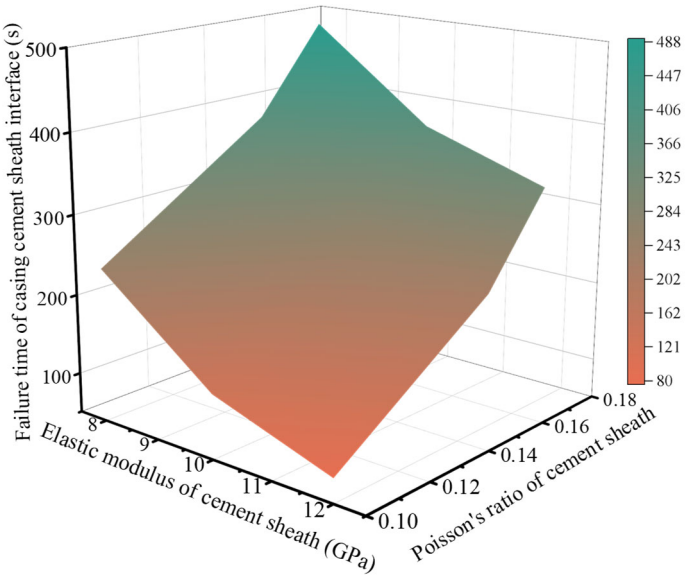

Figure 9. Influence of elastic modulus and Poisson's ratio of cement sheath on failure time of cement sheath

4.3.3. Casing wall thickness

In field construction, casings of various dimensions are encountered. This section investigates the impact of different casing wall thicknesses on the integrity of the cement sheath, with casing wall thicknesses set to 8.8, 10.8, and 12.8 mm. All other parameters are consistent with the baseline case. Fig 10a and 10b respectively illustrate the determination of casing-cement sheath interface failure and the influence of different casing wall thicknesses on the failure time of the cement sheath. They are observed that as the casing wall thickness increases, the time at which failure occurs at the casing-cement sheath interface is delayed. This delay is attributed to the higher load-bearing capacity of thicker casings, which are less prone to deformation, thereby reducing the impact on the casing-cement sheath interface. However, failure still occurred at the interface when the wall thickness was 12.8 mm. To ensure the integrity of the casing-cement sheath-reservoir rock system, thicker casings should be selected, but this may increase costs. Therefore, the decision to use thicker casings to enhance wellbore integrity in the field should be made on a case-by-case basis.

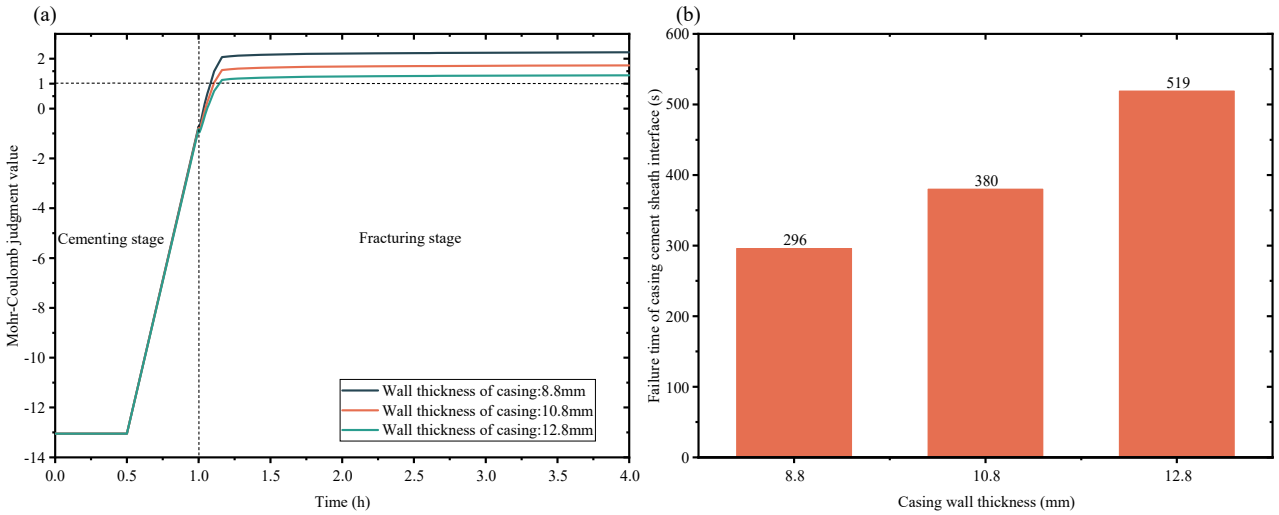

Figure 10. (a) Failure judgment of casing cement sheath interface under different casing wall thickness; (b) Influence of different casing wall thickness on cement sheath failure time

4.3.4. Cement sheath wall thickness

In the field drilling process, irregularities in the wellbore diameter are common[29], and variations in the wellbore diameter, either increases or decreases, can lead to changes in the actual thickness of the cement sheath. Consequently, this section investigates the impact of varying cement sheath wall thicknesses on the integrity of the cement sheath. The wall thicknesses of the cement sheath were set to 15.05, 19.05, and 23.05 mm, while all other parameters remained constant. Fig 11a and 11b respectively depict the assessment of casing-cement sheath interface failure and the impact of varying cement sheath wall thicknesses on the failure time of the cement sheath.. They are observed that, overall, changes in the cement sheath wall thickness have a relatively low impact on its integrity. Regardless of the cement sheath wall thickness, failure at the casing-cement sheath interface occurs with the injection of fracturing fluid.

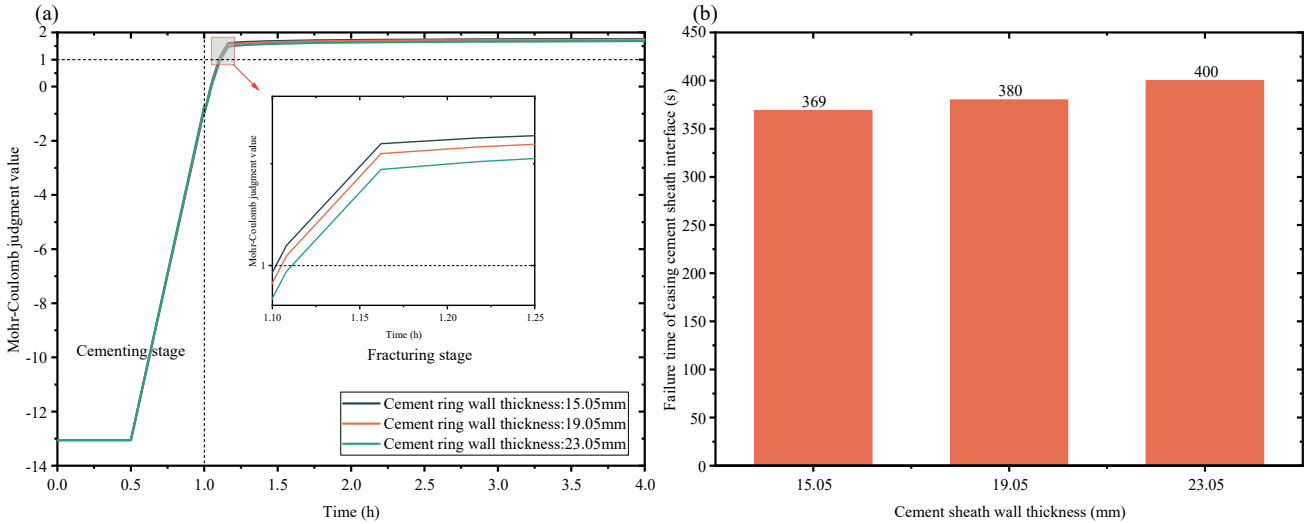

Figure 11. (a) Failure judgment of casing cement sheath interface under different cement sheath wall thickness; (b) Influence of different cement sheath wall thickness on cement sheath failure time

The analysis presented indicates that during the volume modification process of shale gas horizontal wells, employing low-pressure, high-temperature fracturing fluids, selecting cement sheaths with low elastic modulus and high Poisson's ratio, and utilizing casings with greater wall thickness can effectively reduce the risk of failure at the casing-cement sheath interface. This, in turn, enhances the integrity of the casing-cement sheath-reservoir rock system, thereby preventing the fracturing fluid from inducing slippage in faults.

5. Conclusion

This study investigates the mechanism of fault slippage during the hydraulic fracturing process of shale gas horizontal wells and analyzes the causes that induce fault slippage. It is posited that the mechanism of fault slippage is related to the integrity of the cement sheath. A numerical model of the casing-cement sheath-reservoir rock system was established. Numerical simulations were conducted to calculate and analyze the integrity of the cement sheath during the fracturing process, and the impact of fracturing fluid pressure and temperature, the mechanical parameters of the cement

sheath, and the wall thickness of the casing and cement sheath on the integrity were thoroughly investigated. The following conclusions were drawn:

(1) During the fracturing process, low-temperature fracturing fluid causes a decrease in the overall temperature of the casing-cement sheath-reservoir rock system. Radial stresses at both the casing-cement sheath interface and the reservoir rock-cement sheath interface are compressive, while the hoop stress at the casing-cement sheath interface transitions from compressive to tensile, and the hoop stress at the reservoir rock-cement sheath interface remains compressive. Using the Mohr-Coulomb failure criterion to assess both interfaces, it was found that failure at the casing-cement sheath interface occurred approximately 600s after the injection of fracturing fluid, while the reservoir rock-cement sheath interface remained bonded normally.

(2) When the fracturing fluid temperature is 80°C, the cement sheath elastic modulus is 6 GPa, and the cement sheath Poisson's ratio is 0.20 and 0.25, no failure occurred at the casing-cement sheath interface throughout the fracturing stage. This indicates that high-temperature fracturing fluid, low elastic modulus, and high Poisson's ratio of the cement sheath can effectively enhance the integrity of the casing-cement sheath-reservoir rock system. However, the combined effects of different measures require further research.

(3) The entry of fracturing fluid into faults through micro-annuli in the cement sheath is the primary factor inducing slippage in faults located farther from the fracturing area. Enhancing wellbore integrity can effectively prevent fault slippage induced by fracturing fluid.

References

[1] CHEN Zhaowei, ZHOU Wengao, XIANG Degui, et al. Development of rubber composite casing for preventing shale gas casing deformation and its shear resistance evaluation[J]. Natural Gas Industry, 2023(11): 131-136.

[2] HAN Lingling, LI Xizhe, LIU Zhaoyi, et al. Analysis on the causes of casing deformation in fractured shale-gas horizontal wells of Weiyuan Block[J]. Petroleum Exploration and Development, 2023, 50(4): 853-861.

[3] CHEN Zhaowei, XIANG Degui, ZHANG Fengshou, et al. Fault slip and casing deformation caused by hydraulic fracturing in Chang-ning-Weiyuan Blocks, Sichuan: Mechanism and prevention strategy[J]. Petroleum Science Bulletin, 2019, 4(4): 364-377.

[4] Li Y, Liu W, Yan W, et al. Mechanism of casing failure during hydraulic fracturing: Lessons learned from a tight-oil reservoir in China[J]. Engineering Failure Analysis, 2019, 98: 58-71.

[5] GAO Lijun, LIU Zhanli, QIAO Lei, et al. Mechanism Analysis and Numerical Simulation of Casing Failure in Hydraulic Fracturing of Shale Gas Formation[J]. China Petroleum Machinery, 2017, 45(1): 75-80.

[6] Zhang F, Jiang Z, Chen Z, et al. Hydraulic fracturing induced fault slip and casing shear in Sichuan Basin: A multi-scale numerical investigation[J]. Journal of Petroleum Science and Engineering, 2020, 195: 107797.

[7] LI Fanhua, QIAO Lei, TIAN Zhonglan, et al. Analysis on the causes of casing deformation in fractured shale-gas horizontal wells of Weiyuan Block[J]. Oil Drilling & Production Technology, 2019, 41(6): 734-738.

[8] CHEN Ting;CHAI Jian;WANG Zhiqiang, et al. Cause analysis and field treatment of casing damage in shale gas horizontal well volume fracturing[J]. Journal of Shengli College China University of Petroleum, 2020, 34(2): 31-34.

[9] ZHANG Xin;LI Jun; ZHANG Hui; SUN Xiaoming et al. Analysis on Casing Deformation Failure in Deep Shale Gas Wells in Weirong Shale Gas Play[J]. Drilling & Production Technology, 2021, 44(1): 23-27.

[10] LI Jun; ZHAO Chaojie; LIU Gonghui, et al. Assessment of fault slip in shale formation during hydraulic fracturing and its influence factors[J]. Journal of China University of Petroleum(Edition of Natural Science), 2021, 45(2): 63-70.

[11] ZHANG Hui;LI Jun;ZHANG Xiaojun, et al. Leakage path of fracturing fluid into faults and prevention and control measures in shale gas wells[J]. Fault-Block Oil & Gas Field, 2021, 28(6): 750-754+760.

[12] Investigation on dynamic mechanism of fault slip and casing deformation during multi-fracturing in shale gas wells | Scientific Reports[EB].

[13] Wang L, Kwiatek G, Bohnhoff M, et al. Injection-induced fault slip and associated seismicity in the lab: Insights from source mechanisms, local stress states and fault geometry[J]. Earth and Planetary Science Letters, 2024, 626: 118515.

[14] TONG Hengmao;ZHANG Ping;ZHANG Hongxiang, et al. Geomechanical mechanisms and prevention countermeasures of casing deformation in shale gas horizontal wells[J]. Natural Gas Industry, 2021, 41(1): 189-197.

[15] Tian S, Qiao Y, Zhang Y, et al. Analysis of Fault Influence on Geostress Perturbation Based on Fault Model Test[J]. PROCESSES, 2024, 12(6): 1240.

[16] K.c. B, Ghazanfari E, Frash L P. Experimental study of fracture slip due to stress perturbation in fractured geo-resources[J]. Geomechanics for Energy and the Environment, 2023, 33: 100423.

[17] Liu Hao. Research on Horizontal Well Productivity of Shale Gas Reservoir Considering Fault Slip[D]. China University of Petroleum (East China), 2024.

[18] Li Bin. Study of the Casing Failure Mechanism in Horizontal Shale Gas Wells[D]. Southwest Petroleum University, 2019

[19] Yan Xi. Research on Wellbore Integrity Failure Mechanism during Multistage Fracturing in Shale Gas Horizontal Wells[D]. China University of Petroleum(Beijing), 2023.

[20] Song Xixiang. Study on casing deformation in deep shale gas horizontal well under fracturing condition[D]. Chongqing University of Science and Technology, 2023.

[21] Yan Pan. Study on casing deformation in fracturing of shale gas horizontal well[D]. China University of Petroleum(Beijing), 2020.

[22] Zhao Chaojie. Investigation on Failure Mechanism and Test of Casing Deformation in Shale Gas Wells During Multi-Fracturing[D]. China University of Petroleum(Beijing), 2023.

[23] XI Yan;LI Jun;LIU Gonghui, et al. Research into cement sheath integrity during multistage hydraulic fractur-ing in shale gas wells[J]. Petroleum Science Bulletin, 2019, 4(1): 57-68.

[24] Chu Wei;Shen Jiyun;Yang Yunfei, et al. Calculation of micro-annulus size in casing-cement sheath-formation system under continuous internal casing pressure change[J]. Petroleum Exploration and Development, 2015, 42(3): 379-385.

[25] Zeng Bo; Wang Dong; Song Yi, et al. Integrity Analysis of Cement Sheath in Annulus B of Vertical Section during Hydraulic Fracturing[J]. China Petroleum machinery, 2022, 50(8): 89-95.

[26] Gu C, Li X, Feng Y, et al. Numerical investigation of cement interface debonding in deviated shale gas wells considering casing eccentricity and residual drilling fluid[J]. International

Journal of Rock Mechanics and Mining Sciences, 2022, 158: 105197.

[27] Zhou Xiang. Safety analysis on casing and cement sheath during three ultra gas well completion[D]. China University of Petroleum (East China), 2018.

[28] Arjomand E, Bennett T, Nguyen G D. Evaluation of cement sheath integrity subject to enhanced pressure[J]. Journal of Petroleum Science and Engineering, 2018, 170: 1-13.

[29] LOU Erbiao,ZHOU Bo,LIU Hongtao, et al. Effect of Irregular Wellbores on Well Deviation in Air Drilling Through Thick Conglomerate Formations[J]. Petroleum Drilling Techniques, 2021, 49(3): 62-66.